Journal of Sound and Vibration 329 (2010) 880–892

Contents lists available at ScienceDirect

Journal of Sound and Vibration

journal homepage: www.elsevier.com/locate/jsvi

Acoustic response of fibrous absorbent materials to impulsive transient excitations

F. Payri, A. Broatch *, J.M. Salavert, D. Moreno

CMT-Motores Térmicos, Universidad Politécnica de Valencia, Camino de Vera s/n, 46022 Valencia, Spain

ARTICLE INFO

Article history:
Received 24 November 2008
Received in revised form
30 June 2009
Accepted 8 October 2009
Handling Editor: Y. Auregan
Available online 30 October 2009

ABSTRACT

The parameters used to characterize the acoustic behaviour of fibrous absorbent materials are usually the complex characteristic impedance and the complex wavenumber, which permit the calculation of the airflow resistance and vice versa. Different methods have been satisfactorily used by other authors in order to perform this characterization on the basis of a macroscopic modelling of the behaviour of these materials. In this paper, the suitability of this approach for predicting the acoustic response of absorbent materials to impulsive excitations is evaluated. The constant term of the airflow resistance equation for absorbent materials with different densities is quantified by means of a modified version of the impulse method. These values are then incorporated into one-dimensional acoustic calculations in order to predict the response of absorbing materials to pressure pulse excitation. The very good concordance observed between calculated and measured reflection and transmission coefficients shows the suitability of the proposed procedure for the characterization of absorbent materials.

1. Introduction

In the presence of an absorbent material, acoustic waves do not propagate in the same way as in air. If it can be assumed that the solid phase of the material is rigid, only one compression wave propagates and the material can be characterized, from a macroscopic point of view, by its wavenumber and its complex impedance [1]. However, if the solid phase has a finite stiffness, two compression waves and one transversal wave propagate through the material and then the poroelastic model of Biot [2,3] as adapted to the acoustic problem by Attenborough [4] and Allard [5] can be used. The first model is efficient for rigid-frame fibrous materials, whereas the poroelastic model takes into account the interaction between the solid structure and air-filled spaces, thus being suitable for porous materials.

The macroscopic rigid-frame model has been satisfactorily used in many works and its only limitation is related to the type of absorbent material, which must either satisfy the condition of high stiffness of the solid phase, or be one of fibrous type. This model considers that the material can be characterized by two parameters that usually are the wavenumber and the complex impedance. These parameters can be obtained experimentally by means of several procedures. Delany and Bazley [6] carried out an experimental study on a wide range of absorbent materials and obtained various relations for the impedance of the material depending on the frequency and the stationary flow resistance. To obtain the airflow resistance, Ren [7] proposed a method to obtain the dynamic wavenumber, based on the measurement of the transfer function between two signals recorded by microphones located up- and downstream of the test sample, while Woodcock and Hodgson [8] proposed the two-cavity method and the thickness method for poroelastic materials. However, when a precise

* Corresponding author. Tel.: +34 96 387 9650; fax: +34 96 387 7659.
E-mail address: abroatch@mot.upv.es (A. Broatch).

0022-460X/$ - see front matter © 2009 Elsevier Ltd. All rights reserved.
doi:10.1016/j.jsv.2009.10.015

calculation of the acoustic properties of rigid porous materials is required six material parameters should be known, and hence other methods are needed [9].

In thin absorbent rugs for surface covering, the propagation of waves in the material can be modelled by means of a local impedance without considering the propagation of three-dimensional waves. Such a procedure for the assessment of the contribution of the absorbent material in any acoustic system allows its inclusion in a simple way, which is only valid for layered dispositions of the material. In thick absorbent material samples, this simple model is too limited and hence three-dimensional models, that take into account the propagation of the waves in the whole volume of the material, must be considered. In the last few years, the application of modal methods, such as the modal adjustment method for the acoustic analysis of silencers, has won interest. The possibility to dispose of analytical solutions providing high accuracy solutions with a reasonable computational cost is very attractive, even though such solution may be valid only for particular types of silencers. The discretization, such as the finite element method or the boundary element method, for the prediction of the response of these acoustic systems, has several limitations due to the great number of elements required to mitigate the pollution error at medium and high frequencies.

Analytical methods with modal base have been used since the beginning of these studies. For instance, Cummings [10] solved the particular case of a folded annular duct, and Selamet [11–14] provided acoustic solutions with experimental validations for several types of expansion chambers. Recently, Denia, Selamet and Kirby [15] have combined this solution with the finite element method in order to analyse the acoustic attenuation performance of perforated dissipative mufflers with empty inlet/outlet extensions.

In this paper, the suitability of the acoustic solution used by the above mentioned authors is verified through the prediction of the response of the absorbent materials to impulsive excitations. Unlike the usual procedures which make use of either an impedance tube [16,17] or a shock tube [18], in which the reflection properties of sound absorbing materials are measured, a novel methodology allowing for the experimental determination of the different terms in the airflow resistance equation by means of a modified impulse method [19] is proposed. With this purpose, the reflection and transmission coefficients of several samples of absorbent materials were measured. Then, the acoustic response of the absorbent material was predicted by means of a one-dimensional acoustic model and the calculated results were validated with measurements.

The paper is organized as follows. First, a description of the experimental set-up used for the characterization of the absorbent material is given. In Section 3, the theoretical basis of the processing methodology followed for the acoustic characterization of absorbent materials is described. Then, the calculated and measured results are presented and discussed in Section 4. Finally, in the last section, the conclusions obtained from the present study are summarized and possible additional future work is suggested.

2. Experimental set-up

In this work, a modified version of the impulse method [19] was used, in which pressure components carrying information about the acoustical response of fibrous absorbent materials are measured directly in the time domain. In Fig. 1 a scheme of the experimental set-up used for material characterization is given together with a representation of the relevant pressure waves recorded during the tests.

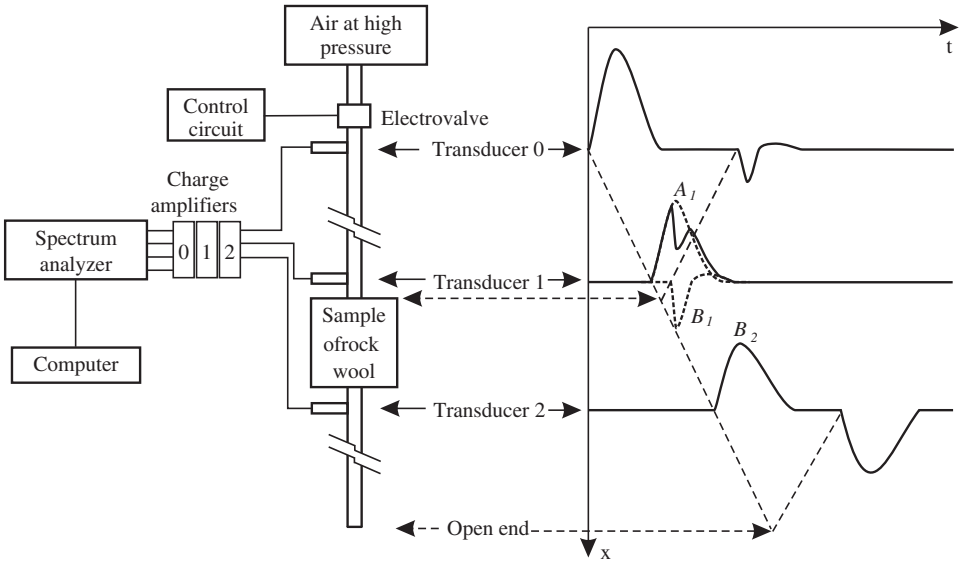

Fig. 1. Scheme of the experimental setup and illustration of relevant pressure components.

The incident pulse is generated by means of a high-speed electrovalve that controls the discharge from a high pressure air tank. A proper choice of the opening time ensures that the spectrum associated with the incident pulse is essentially flat. The length of the ducts located between the valve and transducer 0, transducer 0 and the sample of absorbent material, and the sample and the open end is chosen so that no windowing is necessary in order to isolate the incident, the reflected, and the transmitted pulses, as indicated in the figure. Transducer 0 was located 15 m away from both the valve and the sample of absorbent material, and transducer 2 was placed 0.15 m downstream of the sample, and 15 m away from the open end. However, information on reflection properties as recorded by transducer 0 is highly distorted, due precisely to the huge duct length required to avoid overlapping. This information is only available at points located close to the sample of absorbent material, such as that for transducer 1 in Fig. 1, where it is also indicated that this transducer records the addition of the incident and the reflected pulses. In order to surpass this difficulty, the solution adopted in [19] was to estimate the pulse incident on the sample of absorbent material at Section 1 (whose Fourier transform will give the complex amplitude of the A_1 component) from an additional test performed taking out the sample and using an excitation pulse similar to that recorded by the transducer 0 during the previous test with sample. The pressure pulse recorded by transducer 1 during this additional test is assumed to be the incident pulse that excited the sample in the previous test. Once the incident pulse is so obtained, subtraction from the pressure recorded by transducer 1 in the presence of the sample of absorbent material gives a suitable estimate of the pulse reflected by the sample, whose Fourier transform gives the complex amplitude of the B_1 component. In this way, neither the incident nor the reflected pulse recorded by transducer 0 is used for the absorbent material characterization, so that any effects of wave distortion or of dissipation will not affect the results.

Measurement of the transmitted pulse does not imply any difficulty since it is recorded directly by transducer 2. In fact, the transmitted pulse can be easily isolated by means of time domain windowing with a simple rectangular window. Applying Fourier analysis to the isolated signal the complex amplitude of the B_2 component is obtained.

The scheme of the assembly of the absorbent sample in the measurement location of the impulse test rig is shown in Fig. 2. Here, it can be observed that a certain length of empty duct exists both upstream and downstream of the sample. These lengths are necessary in order to avoid pulse overlapping. Therefore, the reflection and transmission coefficient obtained in the tests are the response of an acoustical system composed of two empty ducts of length 0.15 m (distance between the transducers and the sample of absorbent material) up- and downstream of the sample and a duct portion filled with absorbent material (the sample). Throughout the study the absorbent material used was rock wool, and several samples were tested changing both the density and the thickness of the material.

3. Theoretical basis of processing procedure

In order to consider the presence of absorbent material inside tubes, it is usually assumed that only air exists within the duct, so that the effect the absorbent material is considered through the introduction of an additional friction term in the momentum equation. This additional source term carries information about the airflow resistance, as described by Mechel and Vér [20]. In this way, the effects of the presence of an absorbent material in an acoustic system are represented by a simply resistive term.

As the experimental characterization of the absorbent material was performed by means of the impulse method in cold flow, the hypothesis of isentropic flow can be applied and hence modifications to the energy equation are not required. Similarly, the continuity equation is not modified. Therefore, the assessment of wave propagation through absorbent materials requires the solution of the system of equations formed by the process equation—isentropic, in this case—and the usual equations of mass and energy conservation, together with a momentum equation of the form:

$$\frac{\partial u}{\partial t} + u\frac{\partial u}{\partial x} + \frac{1}{\rho}\frac{\partial p}{\partial x} + R_f\frac{u}{\rho} = 0 \tag{1}$$

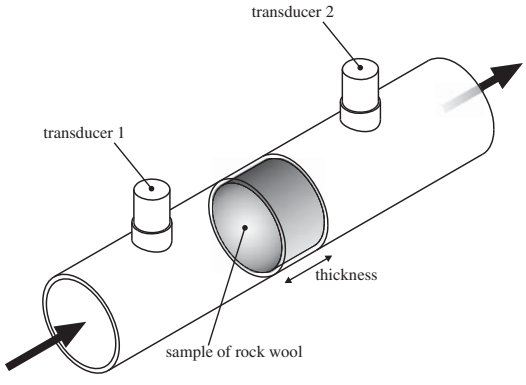

Fig. 2. Scheme of the assembly of the absorbent sample in the measurement place of the impulse test rig.

The fourth term in this expression is the source term accounting for the friction caused by the interaction between the flow and the absorbent material. This term is proportional to the flow velocity fluctuation u and the flow resistivity R_f, and is defined as follows [20,21]:

$$R_f = \frac{1}{1000}\frac{\eta}{\langle r_m^2 \rangle} a\mu^b + c\left(\frac{1}{1000}\frac{\eta}{\langle r_m^2 \rangle} a\mu^b\right)^d |u| \tag{2}$$

where η is the dynamic viscosity of air, $\langle r_m^2 \rangle$ is the mean square average of the fibre radius and μ is the massivity of the absorbent material defined as $\mu = \rho_A/\rho_M$ (being ρ_A the bulk density of the porous absorbent material and ρ_M the density of the fibrous material). The coefficients a, b, c and d are available in the literature [20,21], and are constant and dependent on the material type. Therefore, Eq. (2) can be re-written in short as

$$R_f = \psi + \chi|u| \tag{3}$$

which is similar to Forchheimer's relationship [22–24].

Expressing the flow velocity u as the sum of a mean and a fluctuating component ($u = U + u'$) and assuming that the mean velocity of the gas is zero ($U = 0$), when the combination of Eqs. (1) and (3) is linearized, the pressure and velocity fluctuations are related by the following expressions:

$$-\frac{\partial p}{\partial x} = \mathrm{j}\omega u \rho_0 + \psi u' \tag{4}$$

$$-\frac{\partial u'}{\partial x} = \mathrm{j}\frac{\omega p}{\rho_0 a_0^2} \tag{5}$$

where a_0 stands here for the speed of sound and ρ_0 is the air density.

Using now the mass flow fluctuation $v = \rho S u'$, where S denotes the section and the prime has been dropped for brevity, from these linearized equations, the transfer matrix of a duct filled with absorbent material is finally written as follows:

$$\begin{bmatrix} p_1 \\ v_1 \end{bmatrix} = \begin{bmatrix} \cos(\tilde{K}l) & j\tilde{Z}sen(\tilde{K}l) \\ j\frac{1}{\tilde{Z}}sen(\tilde{K}l) & \cos(\tilde{K}l) \end{bmatrix} \cdot \begin{bmatrix} p_2 \\ v_2 \end{bmatrix} \tag{6}$$

where the complex wavenumber $\tilde{K}$ and complex impedance $\tilde{Z}$ are defined as

$$\tilde{K} = K_0\left(1 - \mathrm{j}\frac{\psi}{\omega\rho_0}\right)^{1/2} \tag{7}$$

$$\tilde{Z} = Y_0\left(1 - \mathrm{j}\frac{\psi}{\omega\rho_0}\right)^{1/2} \tag{8}$$

where K_0 and Y_0 are the wavenumber and the characteristic impedance of air, respectively.

These expressions are consistent with those available in the literature. In fact, using a characteristic impedance and a propagation coefficient (wavenumber) was proposed by Delany and Bazley [6], whereas Lehringer [25] derived the propagation coefficient from both a complex speed of sound and a complex density.

The next step of the proposed procedure deals with the determination of the expressions for the calculation of the "complex wavenumber" and the "complex impedance" from the measured transmission and reflection coefficients. Therefore, relations between these coefficients and the constant term ψ of the airflow resistance R_f must be established, so that the acoustic behaviour of absorbent materials can be predicted through models in either the time or frequency domains.

As was indicated in the previous section, the tests performed in the impulse test rig provide the transmission and reflection coefficients of a system consisting of an empty inlet duct, a duct housing the absorbent material and a final outlet duct. Therefore, the characterization of the absorbent material requires the matrix decomposition of the system. According to acoustic theory, the pressure fluctuation at a given point n (p_n), can be calculated as the linear superposition of two pressure perturbations that propagate in opposite directions, i.e.,

$$p_n = A_n + B_n \tag{9}$$

where A_n and B_n are the progressive and regressive components, respectively, at point n.

For the mass flow fluctuation v_n, the following equation can be formulated:

$$v_n = \frac{A_n - B_n}{Z_n} \tag{10}$$

where Z_n is the characteristic impedance of the propagation medium at point n.

The relation between the forward and backward pressure amplitudes upstream (denoted by 1) and downstream (denoted by 2) of a two-port acoustic element is established by its dispersion matrix [S], which can be expressed as [26]

$$\begin{bmatrix} A_1 \\ B_1 \end{bmatrix} = \begin{bmatrix} S_{11} & S_{12} \\ S_{21} & S_{22} \end{bmatrix} \cdot \begin{bmatrix} A_2 \\ B_2 \end{bmatrix} \tag{11}$$

In addition, the relation between pressure components up- and downstream of the element through the reflection (R) and transmission (T) coefficients in direct and reverse flow [27] can be written in matrix form as with

$$\begin{bmatrix} A_2 \\ B_1 \end{bmatrix} = \begin{bmatrix} T_D & R_R \\ R_D & T_R \end{bmatrix} \cdot \begin{bmatrix} A_1 \\ B_2 \end{bmatrix} \tag{12}$$

In this equation, subscripts D and R refer to direct and reverse flow, respectively. Combining Eqs. (11) and (12), the terms of the dispersion matrix can be expressed as a function of the reflection and transmission coefficients:

$$S_{11} = \frac{1}{T_D} \tag{13}$$

$$S_{21} = \frac{R_D}{T_D} \tag{14}$$

Since the samples of absorbent material are symmetric, the reverse flow tests provided similar results to those obtained in the direct flow tests. Then, since $T_D = T_R$ and $R_D = R_R$, the rest of the terms of the dispersion matrix can be determined as

$$S_{12} = -\frac{R_D}{T_D} \tag{15}$$

$$S_{22} = \frac{T_D^2 - R_D^2}{T_D} \tag{16}$$

In summary, the dispersion matrix of any two-port acoustic element can be determined through the measured reflection and transmission coefficients by using Eqs. (13)–(16). The dispersion matrix of the portion of duct housing the absorbent material can then be obtained extracting from the measured dispersion matrix the contribution of the empty ducts located up- and downstream of the sample. To quantify the contribution of the empty ducts, the well-known dispersion matrix of a duct with section S and length l can be used. Thus,

$$\mathbf{S}_d = \begin{bmatrix} e^{jkl} & 0 \\ 0 & e^{-jkl} \end{bmatrix} \tag{17}$$

where k is the wavenumber. Therefore, the dispersion matrix of the duct with absorbent material can be calculated as follows:

$$\mathbf{S}_a = \mathbf{S}_{di}^{-1} \cdot \mathbf{S}_m \cdot \mathbf{S}_{do}^{-1} \tag{18}$$

being $\mathbf{S}_a$ the dispersion matrix of the absorbent sample, $\mathbf{S}_m$ the measured matrix of the whole system and, $\mathbf{S}_{di}$ and $\mathbf{S}_{do}$ the matrices of the inlet and outlet duct, respectively. Using the well-known relation between the transfer and dispersion matrixes [27], the transfer matrix of the absorbent sample defined by Eq. (6) can be calculated from the terms of the dispersion matrix previously obtained as

$$\begin{bmatrix} T_{11} & T_{12} \\ T_{21} & T_{22} \end{bmatrix}_a = \begin{bmatrix} \cos(\tilde{K}l) & j\tilde{Z}sen(\tilde{K}l) \\ j\frac{1}{\tilde{Z}}sen(\tilde{K}l) & \cos(\tilde{K}l) \end{bmatrix}_a = \frac{1}{2} \cdot \begin{bmatrix} (S_{11}+S_{21}+S_{12}+S_{22}) & Z_2(S_{11}+S_{21}-S_{12}-S_{22}) \\ \frac{1}{Z_1}(S_{11}-S_{21}+S_{12}-S_{22}) & \frac{Z_2}{Z_1}(S_{11}-S_{21}-S_{12}+S_{22}) \end{bmatrix}_a \tag{19}$$

Consider the case of a uniform duct, where inlet and outlet impedances (Z_1 and Z_2) are equal to Y_0. A new expression for the complex impedance—that characterizes the presence of the absorbent material—as a function of the dispersion matrix terms can be obtained dividing the term T_{12}^a by the term T_{21}^a of the two matrices at the right side of Eq. (19). That is,

$$\tilde{Z} = Y_0 \left(\frac{S_{11}^a - S_{12}^a + S_{21}^a - S_{22}^a}{S_{11}^a + S_{12}^a - S_{21}^a - S_{22}^a} \right)^{1/2} \tag{20}$$

Similarly to Eqs. (7) and (8), the complex wavenumber must be

$$\tilde{K} = K_0 \left(\frac{S_{11}^a - S_{12}^a + S_{21}^a - S_{22}^a}{S_{11}^a + S_{12}^a - S_{21}^a - S_{22}^a} \right)^{1/2} \tag{21}$$

Since the scattering matrix can be experimentally obtained from the measured reflection and transmission complex coefficients, both the complex impedance and the complex wavenumber can be also experimentally estimated with Eqs. (20) and (21). Furthermore, the term ψ which, according to Eq. (3), is the constant part of the airflow resistance in a

linear system, can also be determined by equating Eq. (8) to Eq. (20). Assuming that the real parts of both equations are the same, one has

$$\psi = -\omega\rho_0 \,\mathrm{Im}\left(\frac{S_{11}^a - S_{12}^a + S_{21}^a - S_{22}^a}{S_{11}^a + S_{12}^a - S_{21}^a - S_{22}^a}\right) \tag{22}$$

In this way, Eq. (22) permits the experimental estimation of the value of ψ under the hypothesis given before. Then, the characteristics of wave propagation through absorbent materials can be assessed by means of the complex impedance and wavenumber determined with Eqs. (7) and (8). With these parameters, the transfer matrix of a duct filled with absorbent material can be calculated from Eq. (6). This matrix can then be used in combination with any additional transfer matrix in order to perform linear acoustic calculations of more complex systems where absorbing materials are present and, in particular, to the system considered in this study (the absorbent sample together with the connecting upstream and downstream ducts). One-dimensional modelling of this system thus provides values for the complex transmission and reflection coefficients of the system, which can be validated by comparison with those measured in the impulse test rig. Such comparison will provide a check for the validity of the hypothesis used assumed in the macroscopic acoustic model of the absorbent materials when applied to the particular case of pulsed flow.

4. Results and discussion

Several samples of the rock wool with two bulk densities, 100 and 150 kg/m^3, and three thicknesses per density, 30, 40 and 50 mm, have been tested. Samples of 51 mm diameter in a cylindrical duct were considered. The average air temperature during tests was 27 °C, in which the speed of sound is about 345 m/s.

In this section, the impulsive response of the absorbent material is first analysed in the time domain. Then, the coefficient ψ of the airflow resistance is quantified and its dependency with the length and the density of the absorbent material is evaluated. Finally, in the last subsection, the suitability of a one-dimensional model incorporating the equations derived with the proposed procedure for assessing the contribution of absorbent materials is experimentally verified.

4.1. Impulsive response analysis

Fig. 3 shows the incident, reflected and transmitted waves (given in absolute pressure) measured in the impulse test rig for the case of two samples with 150 kg/m^3 density and 30 and 50 mm thick. This figure shows that the reflection is a pressure wave with considerable amplitude, whereas the transmitted wave is very small. This result indicates that the acoustic behaviour of absorbent materials is quite similar to a semi-closed end. In addition, these results also evidence that the amplitude of the reflected and transmitted waves is sensitive to sample thickness. The reflected wave amplitude increases and consequently the transmitted wave decreases as the thickness of the sample increases.

Another important aspect is the bulk density influence on wave propagation. In Fig. 4, the pressure waves measured in tests of samples with 40 mm thick and bulk densities of 100 and 150 kg/m^3 are compared. The effect produced when the bulk density increases is very similar to the effect of an increase in sample thickness. That is, the amplitude of the reflected wave increases and the amplitude of transmitted wave decreases as the packing density of the absorbent material increases.

4.1.1. Airflow resistance assessment

In this section the constant term ψ of the resistivity equation is quantified for all the materials tested using the procedure described in Section 2.

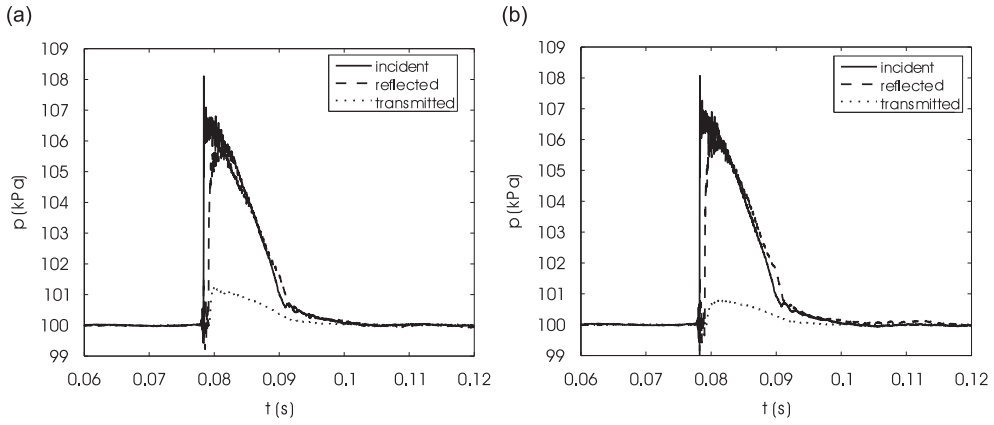

Fig. 3. Incident, reflected and transmitted waves characteristic of a 150 kg/m^3 density sample: (a) 30 mm thick, and (b) 50 mm thick.

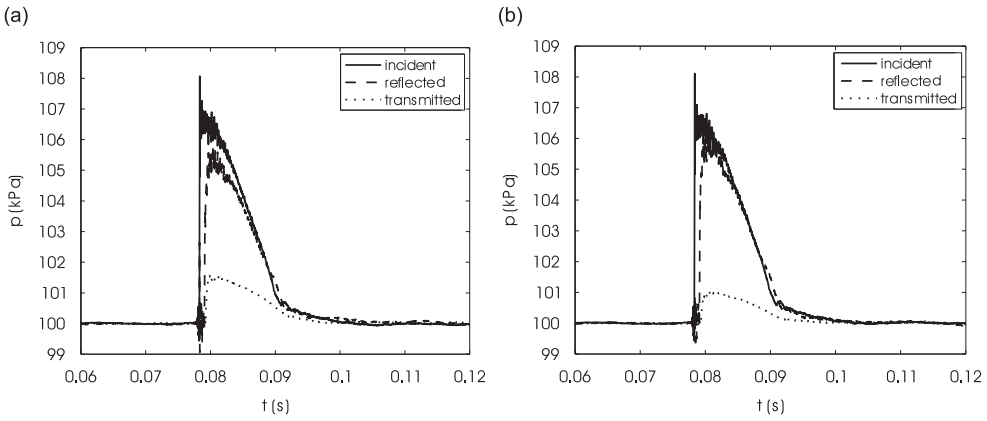

Fig. 4. Incident, reflected and transmitted waves characteristic of a 40 mm thick sample: (a) 100 kg/m^3 density, and (b) 150 kg/m^3 density.

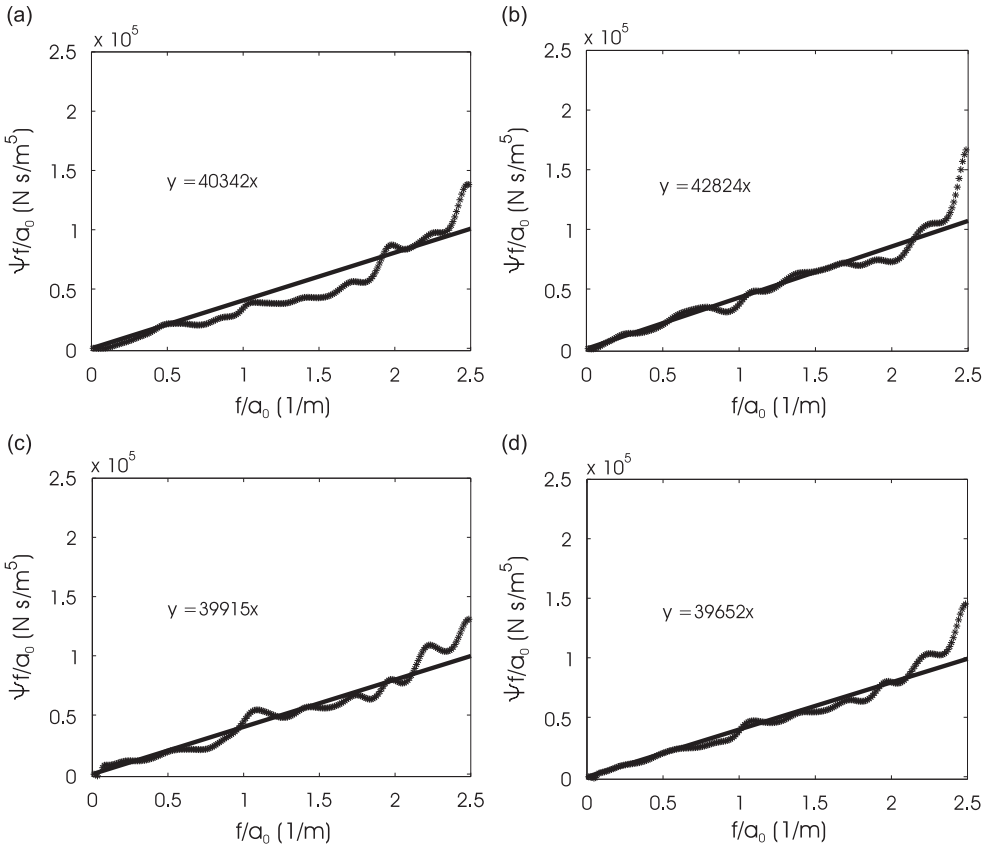

Fig. 5. Airflow resistance term ψ per unit of length of a sample of rock wool with 100 kg/m^3 bulk density: (a) 30 mm thick, (b) 40 mm thick, (c) 50 mm thick, and (d) average value.

First, the results of all samples of absorbent material with a bulk density of 100 kg/m^3 are shown in Fig. 5. Figs. 5a–c show the results obtained from testing samples with the three different thicknesses and Fig. 5d illustrates the arithmetic average value of the previous results as a representative value of the constant part of the airflow resistance of rock wool materials with 100 kg/m^3 density. In these plots, the value of ψ multiplied by the normalized frequency f/a_0 is represented against the normalized frequency. In addition, the least square fit of the measured data is included both graphically and algebraically in each plot. This type of representation permits to diagnose and determine directly the value of ψ by observing the slope of the fit.

In all the cases, the product $\psi f/a_0$ shows a monotonic increase almost proportional to f/a_0. Furthermore, the results also show a quite similar value of ψ in the three cases evaluated, which should indicate that the constant term of the airflow resistance is not sensitive to the absorbent thickness. Considering the average results, the value of the constant part of the airflow resistance ψ for rock wool absorbent with 100 kg/m^3 density can be estimated about 40 000 N s/m^4 with 93 percent of correlation and a mean error of 12 percent.

The results obtained for the samples of rock wool material with 150 kg/m^3 density are shown in Fig. 6. As in the previous case, the results obtained for the different thicknesses are again very similar, so that same comments are applicable also in this case, except that the trends are not so linear. As expected, the value of ψ in this case is higher and it can be estimated about 73 000 N s/m^4 with 96 percent of correlation and a mean error of 10 percent.

The trends observed in Figs. 5 and 6, and the two values of airflow resistance obtained for rock wool material with the proposed procedure are similar to those obtained by Delany and Bazley [6] for fibrous absorbing materials. In addition, the variation of the airflow resistance obtained when the bulk density of the absorbent material changes is also consistent with the results observed by Castagnède et al. [28,29].

4.1.2. One dimensional model validation

In order to perform a first validation of the model of wave propagation in absorbent materials using the ψ values obtained previously, the normalized specific characteristic impedance of the material (ratio between the characteristic complex impedance of the absorbent material and the characteristic impedance of the air) was experimentally and theoretically determined and compared.

The results obtained for the samples of absorbent material with 100 and 150 kg/m^3 density and 50 mm thick are shown in Figs. 7a and b, respectively. These results show good concordance between measurements and calculations in both real and imaginary parts of the impedance ratio. Moreover, better concordance is also evidenced for the sample of lower density at all frequencies.

The larger discrepancies in the case with higher bulk density are localized in very low frequencies ($f/a_0 < 0.75$), whereas for medium and high frequencies the differences are not critic. These results suggest that nonlinear effects, which have not been considered by the model, could be the reason for these discrepancies. In order to investigate the possible nonlinear

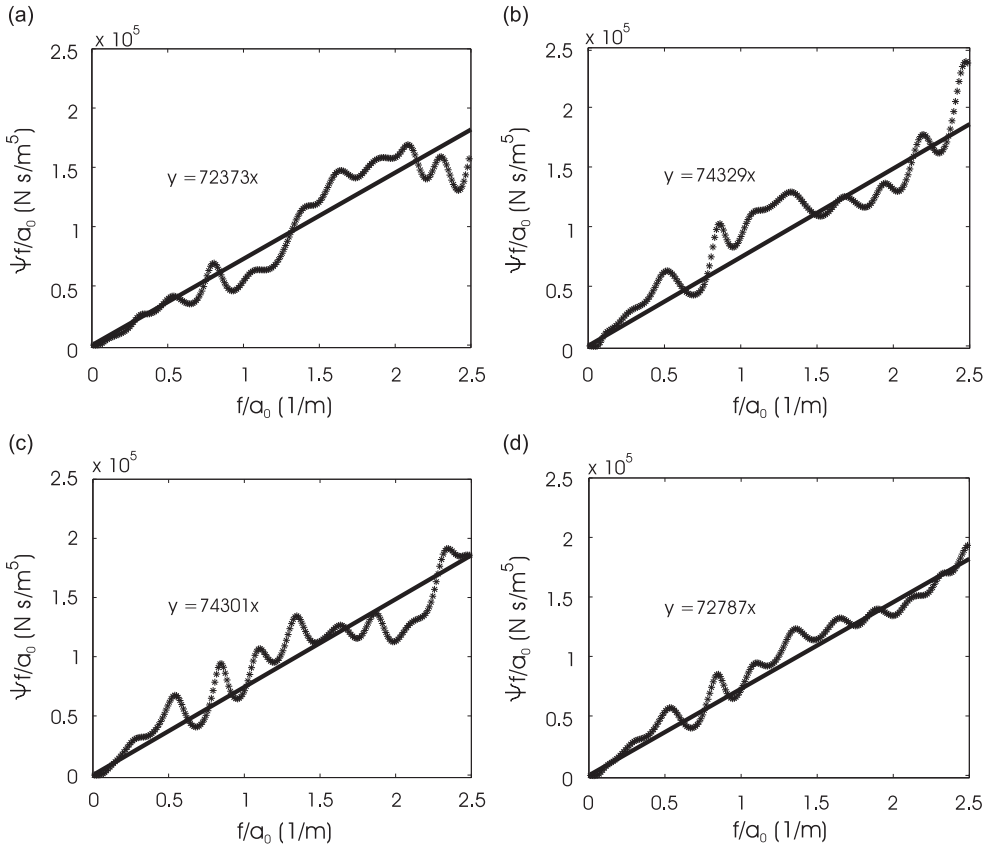

Fig. 6. Airflow resistance term ψ per unit of length of a sample of rock wool with 150 kg/m^3 bulk density: (a) 30 mm thick, (b) 40 mm thick, (c) 50 mm thick, and (d) average value.

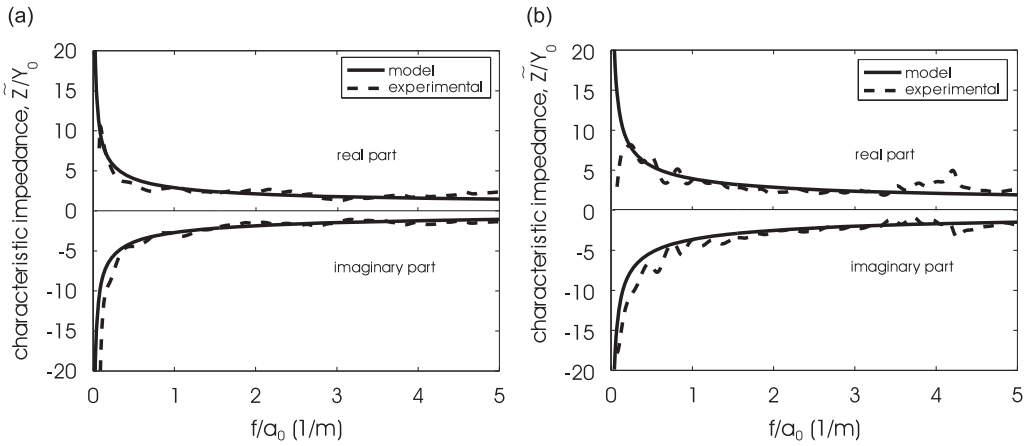

Fig. 7. Normalised specific characteristic impedance of a 50 mm thick sample: (a) 100 kg/m^3 density, (b) 150 kg/m^3 density.

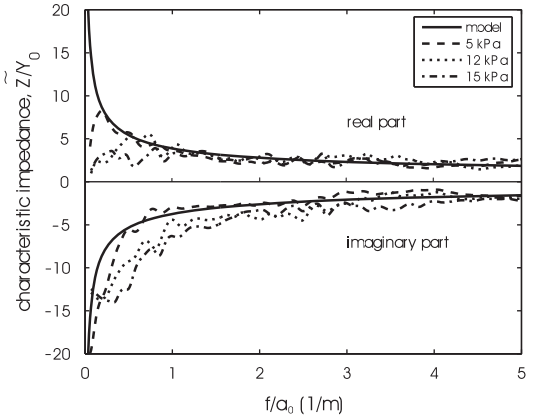

Fig. 8. Sensitivity of the normalised specific characteristic impedance of a 50 mm thick sample of rock wool with 150 kg/m^3 density to incident pressure pulse amplitude.

effects on samples with this density, further tests were performed to evaluate the influence of the incident pressure amplitude on the flow resistivity. With this aim, three incident pulses of different excitation amplitude (5, 12 and 15 kPa) were considered.

Fig. 8 shows the calculated and measured characteristic impedance $\tilde{Z}/Y_0$. In this case, the calculated characteristic impedance value has been obtained considering the previous value of ψ. This figure shows that the model predicts correctly the behaviour of the absorbent materials for the lowest excitation level from a normalized frequency $f/a_0 > 0.5$. Also, it can be observed that when the amplitude of the incident pressure pulse is increased the scatter between measured and calculated characteristic impedance is higher. This can be due to the fact that the mean velocity of the gas has been assumed to be zero and that the proposed model is based on the linearized solution of the combination of Eqs. (1) and (3). These results are consistent with the works of Umnova et al. [22–24], where it is concluded that these nonlinear effects can be assessed with Forchheimer's relationship. This behaviour indicates that certain limitations of the proposed model could arise either when densities higher than 150 kg/m^3 are analysed or when high amplitude pressure pulses are used.

Once the ψ term of the airflow resistance was quantified, one-dimensional modelling of the acoustic response of absorbent materials was also experimentally validated. With this purpose, the complex reflection and transmission coefficients of the system shown in Fig. 2 was calculated with the linear model described in Section 3. Figs. 9 and 10 show the results obtained for samples with the lowest density (100 kg/m^3) and 30 and 50 mm thick, respectively. In these figures the calculated and measured real and imaginary parts of the reflection and transmission coefficients are compared.

The very good agreement between calculated and measured results obtained in the three cases demonstrates the suitability of the proposed model for the description of wave propagation in fibrous absorbent materials. These results show that the thickness of the absorbent material strongly affects the amplitude and frequency location of the transmission

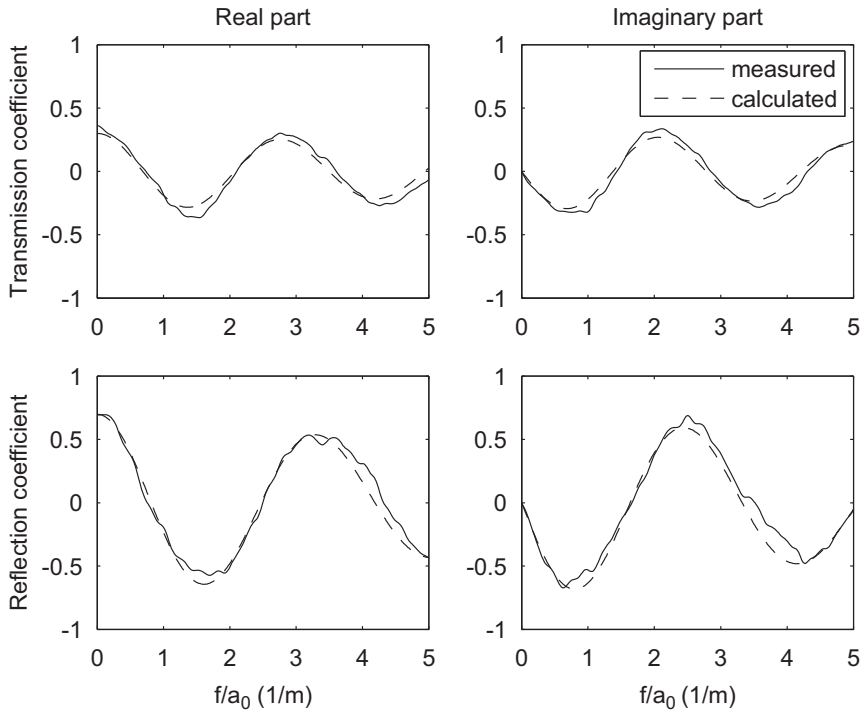

Fig. 9. Reflection and transmission coefficients of a 30 mm thick sample with 100 kg/m^3 density: measured (solid) and calculated (dash).

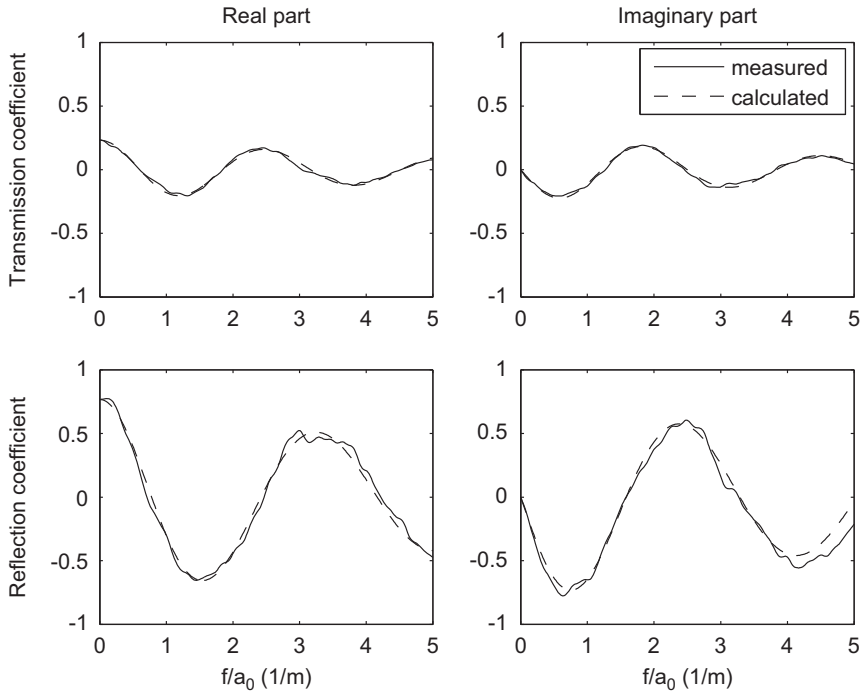

Fig. 10. Reflection and transmission coefficients of a 50 mm thick sample with 100 kg/m^3 density: measured (solid) and calculated (dash).

coefficient peaks, while the reflection coefficient appears to be scarcely sensitive to this variation. The amplitude of the transmission coefficient peaks decreases and are shifted towards low frequencies as the absorbent material is wider. In order to illustrate better this effect, the calculated amplitude and phase of both coefficients are shown in Fig. 11. It is clear

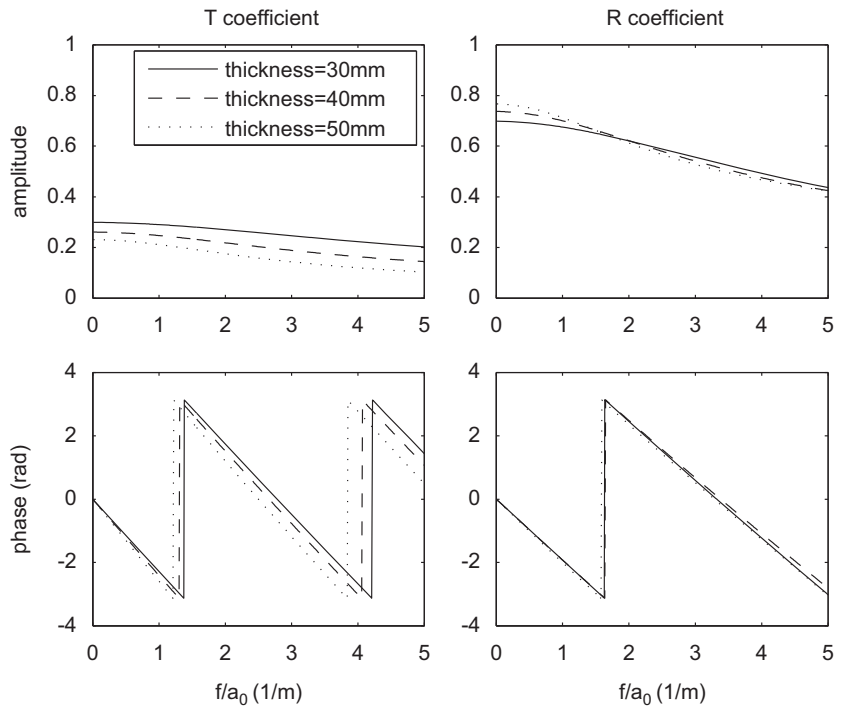

Fig. 11. Effect of sample thickness on the amplitude and the phase of reflection and transmission coefficients of absorbent material with 100 kg/m^3 density.

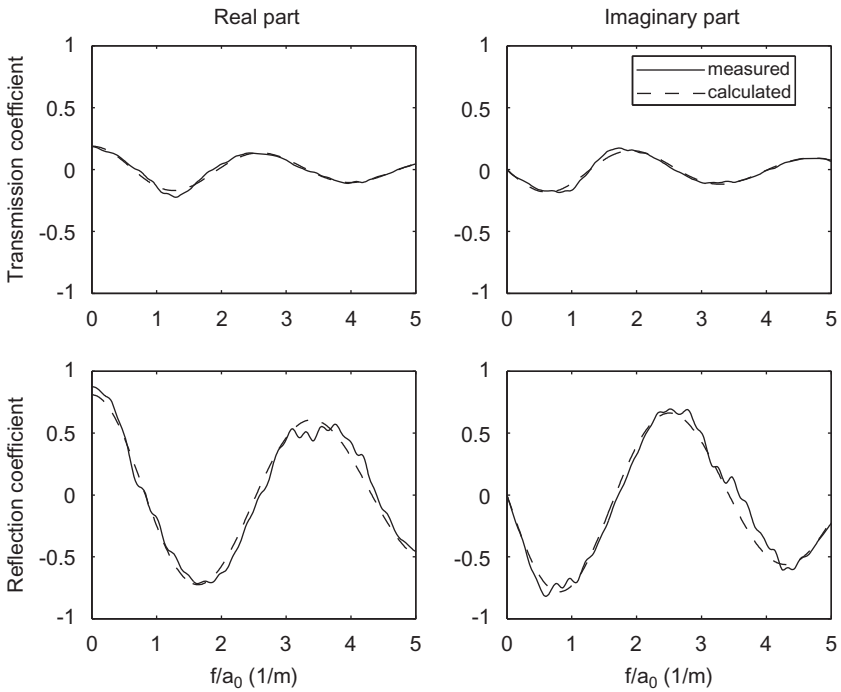

Fig. 12. Reflection and transmission coefficients of a 30 mm thick sample with 150 kg/m^3 density: measured (solid) and calculated (dash).

that the amplitude of the transmission coefficient decreases as the thickness increases, while its phase shifts to lower frequencies. The amplitude of the reflection coefficient is scarcely increased and a non-substantial modification is observed in the phase when thickness is increased.

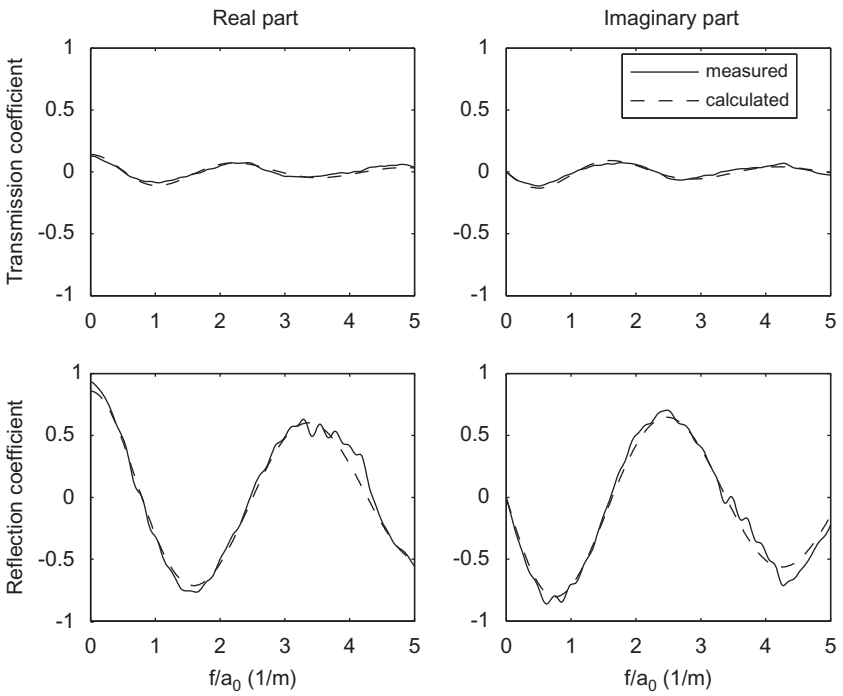

Fig. 13. Reflection and transmission coefficients of a 50 mm thick sample with 150 kg/m^3 density: measured (solid) and calculated (dash).

The results obtained for the samples of 150 kg/m^3 density are shown in Figs. 12, (30 mm thick) and 13 (50 mm thick). These plots show very good agreement between calculations and measurements, even in the low-frequency range despite the discrepancies observed in Fig. 7b, which confirms that the proposed model is still valid for absorbent materials with high bulk density when impulsive excitation is considered. Additionally, with this density, the sensitivity of the transmission and reflection coefficients to material thickness is similar to that observed in the previous case, so that the same comments apply.

In summary, the analysis of the results presented in this section leads to conclude that the macroscopic model of wave propagation in absorbent materials is able to predict the response of acoustic systems containing these materials to impulsive excitations.

5. Conclusions

A novel procedure for the experimental analysis of the acoustic response of fibrous absorbent materials has been proposed in this work. A modified version of the impulse method, which had been previously validated for the characterization of the acoustic response of reactive mufflers, has been adapted so that the constant part of the airflow resistance characteristic and the reflection and transmission coefficients of absorbent materials can be determined.

This airflow resistance constant part resulted to be dependent on the bulk density of the absorbent material, but was not sensitive to the sample thickness. The magnitudes determined for this constant are in agreement with those available in the literature, which have been obtained by using other classical procedures. The results have also shown that for the excitation level used in this study, the airflow resistance scarcely depends on the flow velocity, so that the independent term ψ can be approximated to be the airflow resistance.

A one-dimensional model, based on the equations available in the literature for the macroscopic calculation of the acoustic response of absorbent materials, has been developed. In this model, a resistive term has been included into the momentum equation, so that the effect of the absorbent material on wave propagation could be described. The suitability of the model has been verified measuring the complex reflection and transmission coefficients of a simple system containing absorbent material in the impulse test rig. The very good concordance between calculated and measured results confirm the validity of the model for the prediction of the response to impulsive excitations of elements containing absorbent materials.

Future work should be focused on the validation of the proposed model in more complex acoustic systems, such as dissipative mufflers.

Acknowledgement

This work has been partially supported by Ministerio de Educación y Ciencia through Grant no. PET2006-0301.

References

[1] P.M. Morse, K.U. Inward, *Theoretical Acoustics*, McGraw-Hill, New York, 1968.
[2] M.A. Biot, The theory of propagation of elastic waves in a fluid-saturated porous solid. 1. Low frequency range, *Journal of the Acoustical Society of America* 28 (2) (1956) 168–178.
[3] M.A. Biot, The theory of propagation of elastic waves in a fluid-saturated porous solid. 2. Higher frequency range, *Journal of the Acoustical Society of America* 28 (2) (1956) 179–191.
[4] K. Attenborough, Acoustical characteristics of rigid fibrous absorbents and granular materials, *Journal of the Acoustical Society of America* 73 (3) (1983) 788–799.
[5] J.F. Allard, A. Aknine, C. Depollier, Acoustical properties of partially reticulated foams with high and medium flow resistance, *Journal of the Acoustical Society of America* 79 (6) (1986) 1734–1740.
[6] M.E. Delany, E.N. Bazley, Acoustical properties of fibrous absorbent materials, *Applied Acoustics* 3 (2) (1970) 105–116.
[7] M. Ren, F. Jacobsen, A method of measuring the dynamic flow resistance and reactance of porous materials, *Applied Acoustics* 93 (1993) 265–276.
[8] R. Woodcock, M. Hodgson, Acoustic methods for determining the effective flow resistivity of fibrous materials, *Journal of the Acoustical Society of America* 153 (1) (1992) 186–191.
[9] O. Umnova, K. Attenborough, H.-C. Shin, A. Cummings, Deduction of tortuosity and porosity from reflection and transmission measurements on thick samples of porous materials, *Applied Acoustics* 66 (6) (2005) 607–624.
[10] A. Cummings, Sound transmission in a folder annular duct, *Journal of Sound and Vibration* 41 (3) (1975) 375–379.
[11] A. Selamet, P.M. Radavich, The effect of length on the acoustic attenuation performance of concentric expansion chambers: an analytical, computational and experimental investigation, *Journal of Sound and Vibration* 201 (4) (1997) 407–426.
[12] A. Selamet, Z.L. Ji, Acoustic attenuation performance of circular expansion chambers with offset inlet/outlet: I. Analytical approach, *Journal of Sound and Vibration* 213 (4) (1998) 601–617.
[13] A. Selamet, Z.L. Ji, P.M. Radavich, Acoustic attenuation performance of circular expansion chambers with offset inlet/outlet: II. Comparison with experimental and computational studies, *Journal of Sound and Vibration* 213 (4) (1998) 619–641.
[14] A. Selamet, Z.L. Ji, Acoustic attenuation performance of circular expansion chambers with extended inlet/outlet, *Journal of Sound and Vibration* 223 (2) (1999) 197–212.
[15] F.D. Denia, A. Selamet, F.J. Fuenmayor, R. Kirby, Acoustic attenuation performance of perforated dissipative mufflers with empty inlet/outlet extensions, *Journal of Sound and Vibration* 302 (4–5) (2007) 1000–1017.
[16] V. Panicker, M. Munjal, Impedance tube technology for flow acoustics, *Journal of Sound and Vibration* 77 (4) (1981) 573–577.
[17] M.A. Picard, P. Solana, J.F. Urchueguía, A method of measuring the dynamic flow resistance and the acoustic measurement of the effective static flow resistance in stratified rockwool samples, *Journal of Sound and Vibration* 216 (3) (1998) 495–505.
[18] E. Standley, O. Umnova, K. Attenborough, A. Cummings, P. Dutta, Shock wave reflection measurements on porous materials, *Noise Control Engineering Journal* 50 (6) (2002) 224–230.
[19] F. Payri, J.M. Desantes, A. Broatch, Modified impulse method for the measurement of the frequency response of acoustic filters to weakly nonlinear transient excitations, *Journal of the Acoustical Society of America* 107 (2) (2000) 731–738.
[20] F.P. Mechel, I.L. Vér, Sound-absorbing materials and sound absorbers, in: L.L. Beranek, I.L. Vér (Eds.), *Noise and Vibration Control Engineering*, Wiley, New York, 1992.
[21] R.J. Fairbrother, R. Jebasinski, Development and validation of a computer model to simulate sound absorptive materials in silencing elements of exhaust systems, *IMechE Conference Proceedings: Vehicle Noise and Vibration 2000*, 2000, pp. 331–341.
[22] O. Umnova, K. Attenborough, A. Cummings, High amplitude pulse propagation and reflection from a rigid porous layer, *Noise Control Engineering Journal* 50 (6) (2002) 204–210.
[23] O. Umnova, K. Attenborough, E. Standley, A. Cummings, Behaviour of rigid-porous layer at high levels of continuous acoustic excitation: theory and experiment, *Journal of the Acoustical Society of America* 114 (3) (2003) 1346–1356.
[24] O. Umnova, K. Attenborough, H.-C. Shin, A. Cummings, Response of multiple rigid porous layer at high levels of continuous acoustic excitation, *Journal of the Acoustical Society of America* 116 (2) (2004) 703–712.
[25] F. Lehringer, Modelle zur berechnung von absorptionsschalldämpfern in abgasanlagen (Model for the calculation of absorption mufflers in exhaust system), *MTZ Motortechnische Zeitschrift* 59 (6) (1998) 362–366.
[26] P.O.A.L. Davies, Transmission matrix representation of exhaust system acoustic characteristics, *Journal of Sound and Vibration* 151 (2) (1991) 333–338.
[27] F. Payri, J.M. Desantes, A.J. Torregrosa, Acoustic boundary condition for unsteady one-dimensional flow calculations, *Journal of Sound and Vibration* 188 (1) (1995) 85–110.
[28] B. Castagnède, A. Aknine, B. Brouard, V. Tarnow, Effects of compression on the sound absorption of fibrous materials, *Applied Acoustics* 61 (2) (2000) 173–182.
[29] B. Castagnède, A. Moussatov, D. Lafarge, M. Saeid, Low frequency in situ metrology of absorption and dispersion of sound absorbing porous materials based on high power ultrasonic non-linearly demodulated waves, *Applied Acoustics* 69 (7) (2008) 634–648.